Journal of Applied Polymer Science

Crack growth of natural rubber filled with functionalized silica particles

Aijun Chang,[1,2] Gengsheng Weng,[1,2] Kun Fu,[1,2] Yaxuan Ding,[1,2] Dirong Gong[1,2]

[1]Department of Polymer Science and Engineering, Faculty of Materials Science and Chemical Engineering, Ningbo University, Ningbo 315211, People's Republic of China

[2]Key Laboratory of Specialty Polymers, Ningbo University, Ningbo 315211, People's Republic of China

Correspondence to: G. Weng (E-mail: wenggengsheng@nbu.edu.cn)

ABSTRACT: In the present work, functionalized liquid isoprene rubber (FLIR) was used to improve the filler dispersion and filler–rubber interaction in the silica filled natural rubber system. By the infrared spectra and scanning electron microscopy, it was proved that the FLIR was successfully grafted on the silica and the functionalized silica was dispersed in the NR matrix homogeneously. Based on the real-time crack tip morphology monitoring method, the influence of FLIR on the crack growth behavior of NR filled with silica was analyzed. By the adding of FLIR, the crack resistance of the natural rubber embedded with functionalized silica is remarkably increased. When the weight ratio of FLIR to silica is 3:10, the NR composite has the best crack resistance. © 2015 Wiley Periodicals, Inc. J. Appl. Polym. Sci. **2016**, *133*, 42972.

KEYWORDS: properties and characterization; rubber; structure-property relations

Received 17 June 2015; accepted 23 September 2015

DOI: 10.1002/app.42972

INTRODUTION

Due to the growing demand for the rubber products, the failure of rubber by crack propagation attracts more and more attentions. To enhance the crack resistance, the addition of fillers is an efficient way. As to rubber fillers, silica is of fundamental importance in many rubber applications. However, conventional silica (with polar groups on the silica particle surface) cannot be easily dispersed in the nonpolar rubber such as natural rubber (NR),[1] due to the poor compatibility between silica and NR interface.[2–5] Thus, the dispersion of silica in NR is also of vital importance. To improve the compatibility between silica and NR molecules, an effective way is using coupling agent. At present, the use of silane coupling agent is a popular way.[6] By using silane coupling agent, the compatibility and interface strength can be improved simultaneously. For example, Murakami[3] studied the influence of silane-coupling agent on silica filled natural rubber and found that γ-mercaptopropyltrimethoxysilane (γ-MPS) significantly prevented the delay of sulfur curing and increased the compatibility between NR molecules and silica particles, which improved the mechanical performance of NR vulcanizates. However, very few people paid attention to the functionalized (e.g., carboxyl group) low molecular weight liquid polyisoprene. The functionalized low molecular weight liquid polyisoprene is a kind of new born liquid rubber.[7,8] It has very good compatibility with NR and the function groups provide reaction capacity with silica particles. Moreover, it can also reduce the energy consumption of mixing, participate in the vulcanization process and increase the crosslinking density of rubber vulcanizates.[9] In fact, a similar method has been used in styrene-butadiene rubber system.[10] Thus, it has a great potential for functionalized liquid rubber to improve the crack resistance of silica filled NR.

Nowadays, most studies analyzed crack propagation behavior of rubbers by pure mechanical theories. In recent years, Le Cam *et al.*[11] used an SEM monitoring method to determine the physical mechanism of crack propagation in filled NR. The author also used an original real-time monitoring method to analyze the crack growth mechanism of pure NR and silica filled NR. According to our knowledge, it is a useful method to investigate the influence of silica on the crack resistance of NR. In our previous work, we also used an original real-time monitoring method.[12,13] By this method, the crack growth rate and real-time evolution of crack tip morphology during standard fatigue testing can be recorded. In the present work, the functional liquid isoprene rubber (FLIR) was used and then grafted to silica particle surface to improve the dispersion of silica in NR matrix. The influence of FLIR on the crack growth behavior was investigated by the real-time monitoring method. Finally, we proposed some new insight into the improvement of silica on the crack resistance of NR.

Table I. Recipe of the NR Vulcanizates

Material	Content (phr)
Natural rubber (NR)	100
Zinc oxide	2
Stearic acid	5
Accelerator CZ[a]	1
Sulfur	2
Silica	10
FLIR	Variant

[a] *N*-Cyclo-hexyl-2-benzothiazolesulfenamide.

EXPERIMENTAL

Materials

Natural rubber (NR) used in this work is standard Vietnamese rubber (SVR3L). Functional liquid isoprene rubber (M_n = 4.5 × 10^4 and M_w/M_n = 3) was supplied by Kuraray. Silica with specific surface area of 160 m^{-2} g^{-1} and pH of 6.45 were supplied by Rhodia (Qingdao, China). The particle size of silica is about 30 nm, and the average number of OH group per silica particle, which is measured by titrimetric method, is about 6700. Nonvulcanized NR, including FLIR and silica were mixed in an internal mixer (HAPRO RM-200A). The temperature was held for 10 min in the range of 145–160°C at a rotor speed of 35 rpm to ensure the reaction of the FLIR with silica surface. Then, the FLIR grafted silica compounds (FLIR$_x$-*g*-silica$_y$, where x denotes the fraction of FLIR relative to the silica, and y denotes the fraction of silica) were obtained. Afterwards, the FLIR$_x$-*g*-silica$_y$ together with all the vulcanization ingredients and NR were mixed on a laboratory twin roll mixing mill (SK-160B, made by Shanghai Rubber Machine, China) at room temperature, and then vulcanized at 150°C for 13 min under a pressure of 1.5 × 10^7 Pa. Finally, the FLIR$_x$-*g*-silica$_y$ filled NR vulcanizates (NR/FLIR$_x$-*g*-silica$_y$) were obtained. The recipe of the NR vulcanizates was shown in Table I.

Fourier Transform Infrared Spectroscopy

FTIR analysis was carried out on a Nicolet 6700 Fourier transform infrared spectra (FTIR) spectrometer. The spectral range is 4000–400 cm^{-1}. A resolution of 4 cm^{-1} was chosen. The spectra were obtained with the KBr pellet technique. FLIR and silica were reacted at 120°C in agitation reactor and then finely grounded and mixed with KBr powder.

Vulcanization Characteristics

The cure characteristics of the rubber compounds were measured by a curemeter (GOTECH MD-3000A) at 150°C.

Determination of Crosslink Density

The crosslink density was determined by equilibrium swelling. Specimens were swollen in toluene at room temperature for 72 h and then removed from the solvent, and the toluene on the specimen surface was quickly blotted off with tissue paper. The specimens were immediately weighed on an analytical balance to the tolerance of 1 mg, and then vacuum dried. The crosslink density of the vulcanizates was determined on the basis of the Flory–Rhener[14]:

$$-\left[\ln\left(1-\Phi_r\right)+\Phi_r+\chi\Phi_r^2\right]=V_0M_c\left[\Phi_r^{1/3}-\Phi_r/2\right] \quad (1)$$

where Φ_r is the volume fraction of polymer in the swollen mass, V_0 is the molar volume of the solvent (106.2 cm^3 for toluene), M_c is crosslinking density, χ is the Flory–Huggins polymer–solvent interaction term. The value of χ for toluene – NR is 0.39.The value of Φ_r was reached according to the method used by Bala *et al.*[15]:

$$\Phi_r=\frac{w_2/\rho_2}{\frac{w_2}{\rho_2}+\frac{w_1-w_2}{\rho_1}} \quad (2)$$

where w_1 and w_2 are the weights of the swollen and deswollen specimens, respectively, and ρ_1 and ρ_2 are the densities of the toluene and the cured rubber.

Scanning Electron Microscopy (SEM)

In order to understand the dispersion state of silica in NR, the micromorphologies of the NR vulcanizates were investigated by a SEM instrument (Su-70, Hitachi, Japan) operation at 15 kv. First, 1.0 × 10^5 cycles fatigue loadings at a frequency of 10 Hz were applied to the samples on the DMA + 1000 dynamic mechanical analyzer. Then, the samples were fractured under cryogenic temperature. After freeze fracture, the cross-sections were coated with a thin layer of gold for morphology observation.

Figure 1. Apparatus of fatigue loading test and real-time photographing. [Color figure can be viewed in the online issue, which is available at wileyonlinelibrary.com.]

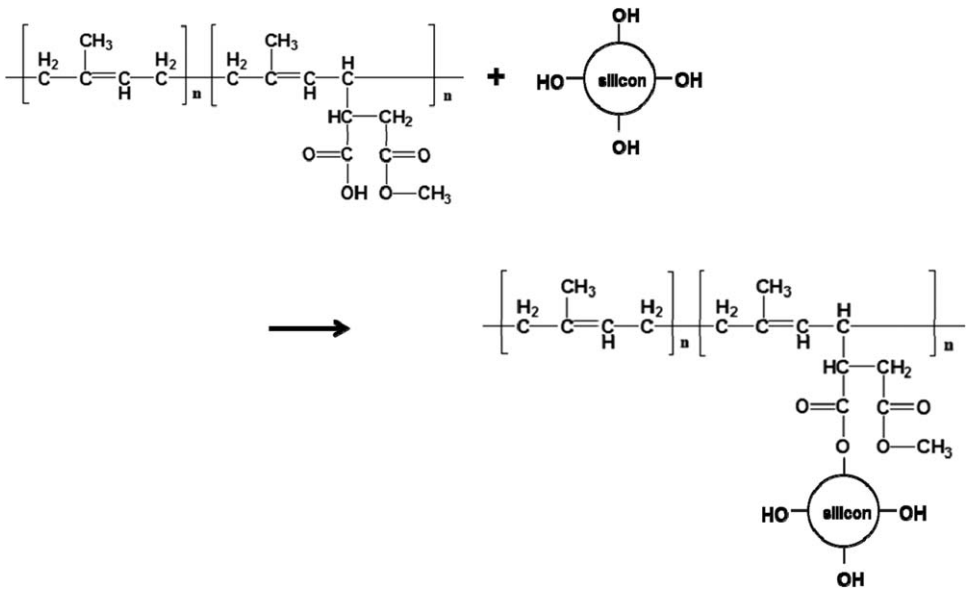

Figure 2. Schematic drawing of re action between silica and FLIR.

Fatigue Loading Test and Real-Time Photographing

For the fatigue loading test, a Metravib DMA + 1000 dynamic mechanical analysis machine had been used, the size of the sample is 2 × 8 × 35 mm. The samples were precut at both sides (see Figure 1)

These tests were carried out at a room temperature with a frequency of 10 Hz. The *T* values were given by the machine computation under the following three steps:

1. Applying a number of excitation cycles to the specimen in order to stabilize it.
2. Calculating the relation automatically between the energy delivered per area unit and loading displacement value and drawing the tear energy (*T*) curve which allows the displacement value to be applied for each cracking *T* value.
3. Choosing the corresponding displacement when the experimental condition is validated.

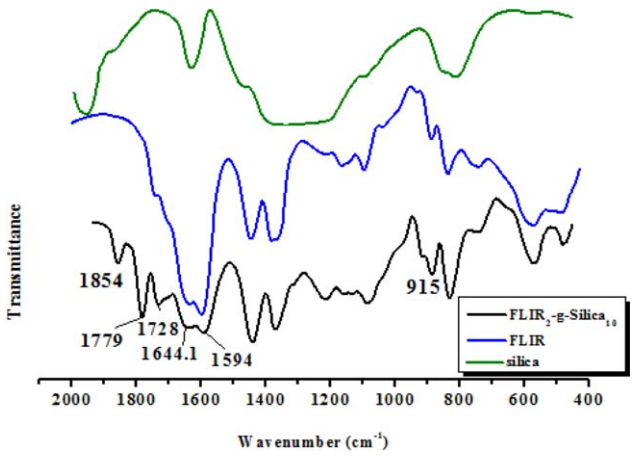

Figure 3. FITR spectra of FLIR, silica and $FLIR_2$-*g*-$silica_{10}$. [Color figure can be viewed in the online issue, which is available at wileyonlinelibrary.com.]

During the tests, the Leica microscope lens in the front was used to locate the crack tip. An ultra-high speed camera (Olympus i-speed 3) was placed on the side. It was employed to photograph the damage zone of crack tip in real time.

RESULTS AND DISCUSSION

Grafting of FLIR on Silica

The functionalized liquid polyisoprene was used in this work bears carboxyl groups (COOH), while silica bears hydroxyl groups (OH) on the surface. Thus, grafting reaction occurs between the hydroxyl groups from silica and the carboxyl groups from FLIR. The reaction mechanism between FLIR and silica can be seen in Figure 2. The FTIR measurement was performed to confirm the grafting of FLIR on to the silica surface. The FTIR results were shown in Figure 3.

Characteristic absorption peaks can be observed in Figure 3. The small peak at 915 cm^{-1} can be assigned to Si—O—Si symmetrical stretching vibration from the existence of silica particles.[11] Two new peaks at 1779 and 1854 cm^{-1} appear. The two peaks can be assigned to the O═C—O(ester group) stretching vibration.[6] It proves the condensation reaction of the carboxylic acid groups and hydroxyl groups successfully happened and the FLIR molecules are successfully grafted on to silica surface. From the FTIR results, we can also see two visible peaks at 1594 and 1644 cm^{-1}, which correspond to the C═O and C—O coupled vibrations of FLIR.[7] Due to the exist of FLIR, the peak at 1728 cm^{-1} is assigned to the O—H bending vibration of hydrate water on the silica surface.[7] Particularly, since FLIR has the same backbone structure with NR, the FLIR grafted silica can participate in the vulcanization process. Thus, silica and NR molecules can be connected by FLIR. Besides, the FLIR grafted silica will be more compatible with the NR matrix.

Cure Characteristics

The cure characteristics data of the rubber composites are given in Table II, and the cure curves are shown in Figure 4. It is seen

Table II. Cure Characteristics of the Rubber Compounds

	t_{s2}/min	t_{90}/min	Tensile strength/MPa	Elongation at break (%)	Crosslink density (mol m^{-3})
NR/silica$_{10}$	5.88	13.80	12.3	406	2.01 × 104
NR/FLIR$_1$-*g*-silica$_{10}$	6.82	14.52	14.6	561	2.32 × 104
NR/FLIR$_2$-*g*-silica$_{10}$	6.92	14.70	14.3	571	2.34 × 104
NR/FLIR$_3$-*g*-silica$_{10}$	6.85	14.40	14.5	583	2.48 × 104
NR/FLIR$_4$-*g*-silica$_{10}$	7.25	15.28	14.1	498	2.53 × 104

ML: minimum torque; MH: maximum torque.
t_{s2}: Time when the minimum torque rise by 0.2 N m.
t_{90}: Time when torque reaches ML + (MH − ML) × 90%.

that with the increasing of the FLIR content, the cure curves shift to the long time side. It indicates that the scorch time of the rubber is extended. When FLIR is added into NR, it participates in the vulcanization process. So, it can be seen that the plateau torque inceases. This result suggests that the crosslinking density (shown in Table II) increases when FLIR-*g*-silica is embedded in NR. The plateau torque reaches a maximum at the FLIR content of 3 phr. Thereafter, plateau torque decreases. Moreover, it can be seen that the tensile strength and elongation at break of rubber compounds has a increasing trend when the FLIR was used. They reach maximum simutaneously at NR/FLIR$_3$-*g*-silica$_{10}$. So, NR/FLIR$_3$-*g*-silica$_{10}$ has the best mechanical properties.

To reveal the influence of FLIR on the vulcanization mechanism, vulcanization kinetics are discussed further. Like many classical chemical reactions, the vulcanization kinetics can be modeled by a differential equation which related to time and temperature, and the equation can be written as follows[16,17]:

$$d\alpha/dt = K(T)f(\alpha) \tag{3}$$

where α is the conversion, $d\alpha/dt$ is the vulcanization rate, t is the time, K is a kinetic constant at temperature T, and $f(\alpha)$ is a function corresponding to the phenomenological model.

If we use the vulcanization curve to study the vulcanization kinetics, we defined α as follows[17]:

$$\alpha = \frac{M_t - M_0}{M_\infty - M_0} \tag{4}$$

where M_0, M_t, and M_∞ are the torque values at time zero, at a given curing time and at the end of the vulcanization process.

Because the vulcanization process is an autocatalytic reaction, so $f(\alpha)$ is listed as follows[17,18]:

$$f(\alpha) = a^m(1-\alpha)^n \tag{5}$$

where $0 \leq m \leq 1$ and $n \geq 1$ are both the orders of reaction. Thus, eq. (1) can be given as 19:

$$d\alpha/dt = K(T)\alpha^m(1-\alpha)^n \tag{6}$$

As it is shown in Figure 5, the experimental data can be well fitted with eq. (6). It indicates that the vulcanization process is not a simple elemental reaction, but various reactions, these reactions are autocatalytic processes during vulcanization. The fitting results are shown in Table III. We can clearly see that K is lower than that of NR at the FLIR content of 1, 2, and 4 phr, while it is slightly higher than that of NR/silica10 at the FLIR content of 3 phr. It is suggested that the vulcanization is first suppressed, then promoted as the FLIR content increases. Finally, vulcanization is suppressed again at

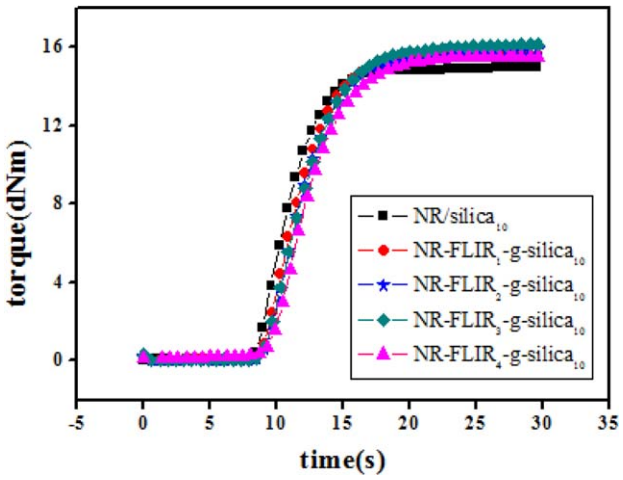

Figure 4. Cure curves of NR with different FLIR$_x$-*g*-silica$_{10}$. [Color figure can be viewed in the online issue, which is available at wileyonlinelibrary.com.]

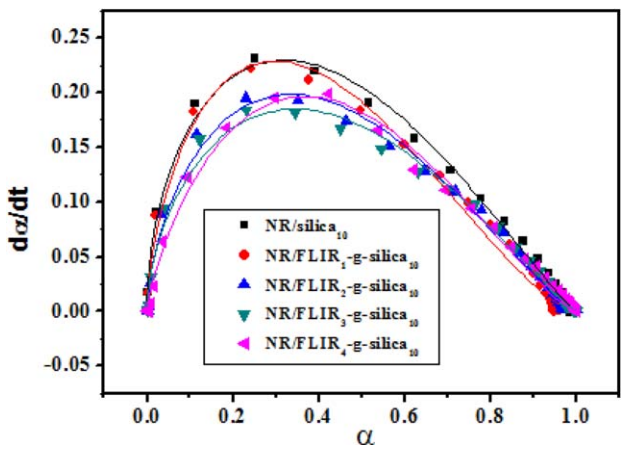

Figure 5. Representative plotting of the $d\alpha/dt$ as a function of α for the NR/silica$_x$-*g*-silica10 composites. The lines are the corresponding fitting curves based on eq. (6). [Color figure can be viewed in the online issue, which is available at wileyonlinelibrary.com.]

Table III. Kinetic Parameters by Fitting the Experimental Data in Figure 4

	K	*m*	*n*	*m* + *n*
NR/silica$_{10}$	0.81	0.80	1.37	2.17
NR/FLIR$_1$-*g*-silica$_{10}$	0.58	0.61	1.17	1.78
NR/FLIR$_2$-*g*-silica$_{10}$	0.67	0.64	1.27	1.91
NR/FLIR$_3$-*g*-silica$_{10}$	0.85	0.64	1.51	2.15
NR/FLIR$_4$-*g*-silica$_{10}$	0.67	0.55	1.16	1.71

the FLIR content of 4 phr. The $m + n$ value of NR/FLIR3-*g*-silica10 is nearly the same with that of NR. It indicates that NR/FLIR3-*g*-silica10 and NR have the same reaction order. The other $m + n$ values of NR/FLIR$_x$-*g*-silica10 are lower than NR, which implies that the reaction order is slightly changed at other FLIR contents.

Dispersion of Silica in Natural Rubber

Figure 6 shows the SEM images of NR/silica$_{10}$ (a) and NR/FLIR$_x$-*g*-silica$_{10}$ (b–e), where $x = 1$, 2, 3, and 4. It is evident that large silica agglomerates exist in NR/silica, indicating poor compatibility between silica and NR matrix. It is known that the silica particle surface has many silicon hydroxyl groups.[20] Therefore, it is easy to agglomerate in the nonpolar NR matrix.[21] So large aggregates exist in the NR matrix in Figure 6(a). When FLIR is grafted on the silica particles, the dispersion state of silica is largely improved [see Figure 6(b–e)]. Particularly, it can be seen that FLIR$_3$-*g*-silica$_{10}$ silica particles have the best dispersion state. This proves that FLIR can enhance the compatibility between silica and NR matrix effectively. Additionally, the worse dispersion of silica for NR/FLIR$_4$-*g*-silica$_{10}$ may be resulted from the aggregation of excessive FLIR.

Crack Growth Rate of Rubber Composites

It is widely accepted that crack growth rate of rubber can be expressed as the following relation[22]:

$$dc/dn = BT^{\alpha}$$

where c is the cracking length, n is the number of loading cycles, T is tear energy, B and α are constants which are related to the material property. The crack growth rates of NR vulcanizates with different FLIR$_x$-*g*-silica$_{10}$ were determined as a function of tearing energy and results are given in Figure 7. By using FLIR, the dc/dn value reaches a minimum at 3 phr FLIR and shows an increasing trend thereafter. It indicates that FLIR grafted silica can decrease the crack growth rate significantly. Additionally, the crack growth rate curve of NR filled with 3 phr *Bis*[3-(triethoxysilyl)propyl]tetrasulfide (Si69) grafted silica (NR/Si69-*g*-silica$_{10}$) is shown in this figure. Obviously, the crack growth rate of NR/FLIR$_3$-*g*-silica$_{10}$ is lower than the NR/Si69-*g*-silica$_{10}$. So, FLIR can promote crack resistance more effectively than Si69 at the same weight percent. To understand the mechanism, Payne effect measurements were performed first and the result is shown in Figure 8. It is seen that the G' values of all the samples show plateaux in strain amplitudes for strain less than 10%. When the FLIR was applied, the plateau modulus increases dramatically, especially for the NR/FLIR$_3$-*g*-silica$_{10}$ and

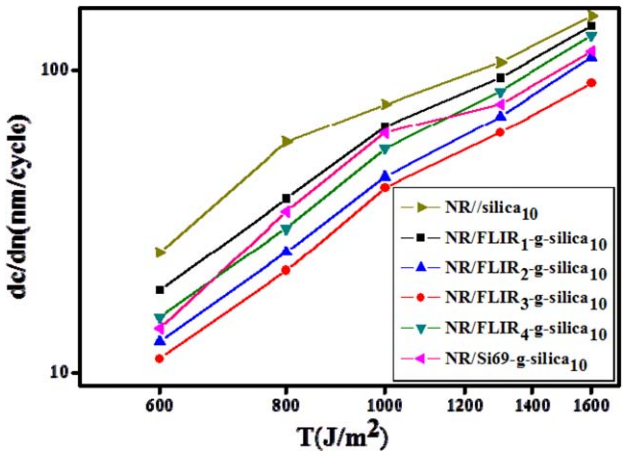

Figure 7. The crack growth rates of silica and FLIR grafted silica filled NR vulcanizates. The crack growth rate curve of NR filled with Si69 grafted silica is shown as a benchmark. [Color figure can be viewed in the online issue, which is available at wileyonlinelibrary.com.]

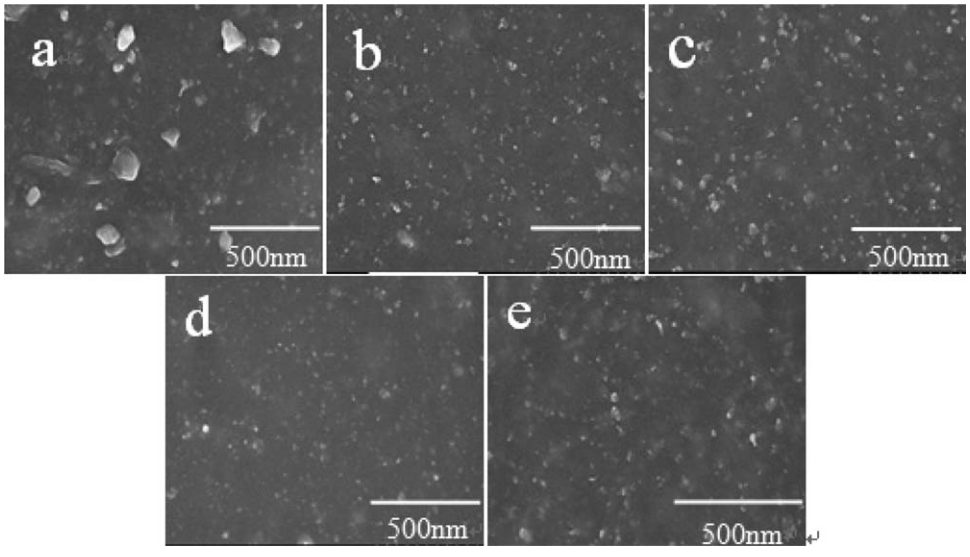

Figure 6. SEM images of (a) NR/silica, (b) NR/FLIR$_1$-*g*-silica$_{10}$, (c) NR/FLIR$_2$-*g*-silica$_{10}$, (d) NR/FLIR$_3$-*g*-silica$_{10}$, and (e) NR/FLIR$_4$-*g*-silica$_{10}$.

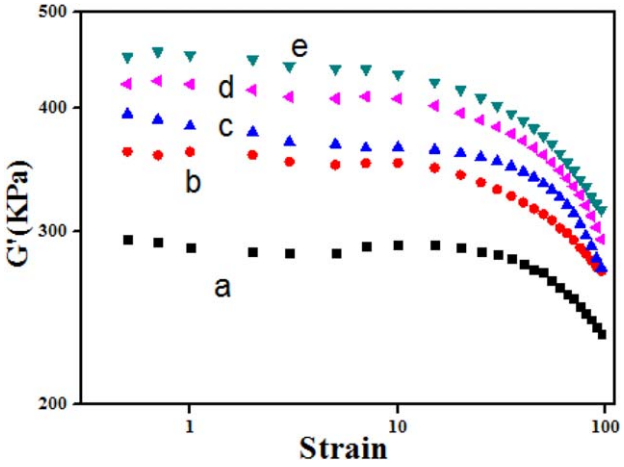

Figure 8. Plots of storage modulus versus strain for silica and FLIR grafted silica filled NR vulcanizates. (a) NR/silica, (b) NR/$FLIR_1$-*g*-$silica_{10}$, (c) NR/$FLIR_2$-*g*-$silica_{10}$, (d) NR/$FLIR_3$-*g*-$silica_{10}$, and (e) NR/$FLIR_4$-*g*-$silica_{10}$. [Color figure can be viewed in the online issue, which is available at wileyonlinelibrary.com.]

NR/$FLIR_4$-*g*-$silica_{10}$, the plateau modulus of NR/$FLIR_3$-*g*-$silica_{10}$ is very close to that of NR/$FLIR_3$-*g*-$silica_{10}$ and their plateau moduli are higher than others. This clearly suggests that the silica network existed in the NR matrix is strengthed significantly. As a result, the enhanced silica network can prevent the crack growth more effectively. So, the crack resistance can be improved.

To further reveal crack resistance mechanism, the crack tip morphologies of the vulcanizates under cyclic loading were recorded. The crack-front morphologies of NR/silica and NR/$FLIR_x$-*g*-$silica_{10}$ captured by high speed microscopic camera are shown in Figure 9. As it is observed in Figure 9, tensile loading direction is indicated in the images and the propagation direction is normal to the photograph. It can be seen that the crack tip is composed of a number of dimple zones separated by ligaments. It is clear that ligaments in Figure 9(d) has the thinnest and most homogeneous distribution on the crack tip (only one thick ligament pointed by the arrow can be seen in panel d). It implies that there are more new surface created for the NR/$FLIR_3$-*g*-$silica_{10}$ sample.[23] It is known that the crack propagation is concerned with cracking surface energy dissipation.[24] So, it indicates that more energy is needed for cracking. According to the above analysis, enhanced silica network is the key to improve the crack resistance. It improves the crack resistance in two ways: the one is the strong filler network which hinders the growth of the crack; the other is the homogeneous silica particles lead to more new surfaces created at the crack tip, which increases the cracking energy consumption.

CONCLUSIONS

In this work, FLIR is grafted on the silica through a simple mixing processing. As a result, the interface bonding between silica and NR is enhanced and silica can be finely dispersed in NR matrix. Fatigue testing proves that FLIR functionalized silica can improve crack resistance significantly and NR filled with $FLIR_3$-*g*-$silica_{10}$ has the best crack resistance. Further analysis proves that enhanced silica network is the key for the improvement on crack resistance. It improves the crack resistance in two ways: the one is the strong filler network which hinders the growth of the crack; the other is the homogeneous silica particles lead to more new surfaces created at the crack tip, which increases the cracking energy consumption. This work gives us a new chance to enhance the crack resistance of rubber.

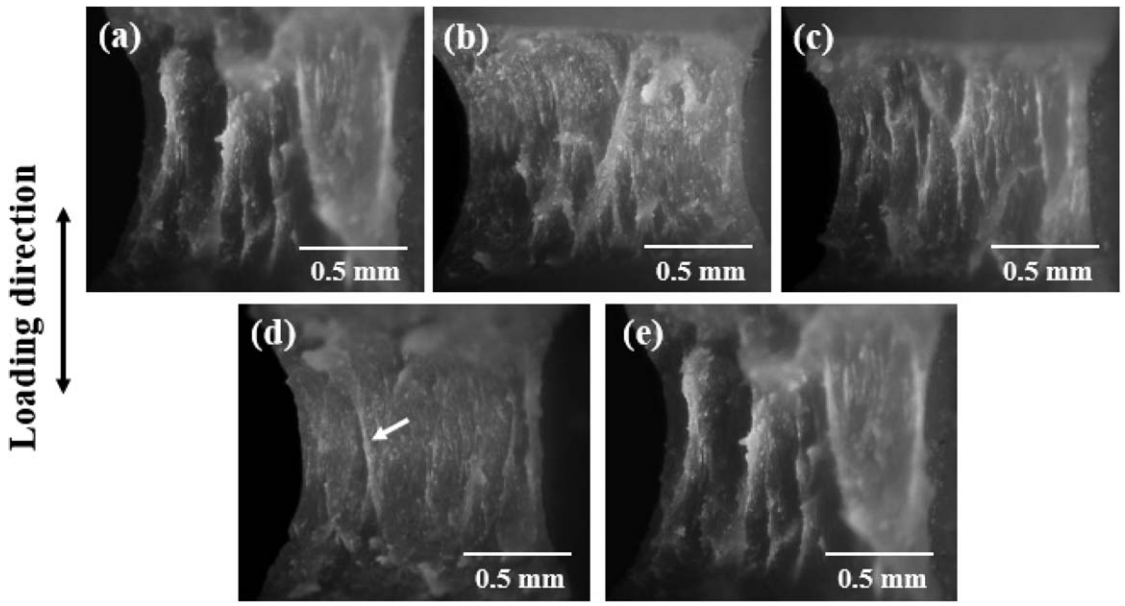

Figure 9. Crack-front morphology of (a) NR/silica, (b) NR/$FLIR_1$-*g*-$silica_{10}$, (c) NR/$FLIR_2$-*g*-$silica_{10}$, (d) NR/$FLIR_3$-*g*-$silica_{10}$, and (e) NR/$FLIR_4$-*g*-$silica_{10}$ tested at $T = 600$ J m^{-2}.

ACKNOWLEDGMENTS

The authors warmly thank the financial support of National Natural Science Foundation of China (Grant No. 21404063), Zhejiang Natural Science Foundation Committee (Grant No. LQ14E030001), Ningbo Municipal Science and Technology Bureau (Grant No. 2013A610024), and the Zhejiang Provincial Education Department (Grant No. Y201327227). The authors are also grateful for Ningbo University.

REFERENCES

1. Meera, A.; Said, S.; Grohens, Y.; Thomas, S. *J. Phys. Chem. C* **2009**, *113*, 17997.
2. Roy, N.; Sengupta, R.; Bhowmick, A. K. *Prog. Polym. Sci.* **2012**, *37*, 781.
3. Yan, H.; Tian, G.; Sun, K.; Zhang, Y.; Zhang, Y. *J Polym. Sci. Pol. Phys.* **2005**, *43*, 573.
4. Rattanasom, N.; Saowapark, T.; Deeprasertkul, C. *Polym. Test.* **2007**, *26*, 369.
5. Choi, S. S. *J Appl. Polym. Sci.* **2002**, *83*, 2609.
6. Qu, L.; Yu, G. *J. Appl. Polym. Sci.* **2012**, *126*, 116.
7. Ma, P. C.; Kim, J. K.; Tang, B. Z. *Carbon* **2006**, *44*, 3232.
8. He, X. J.; Chen, H.; Kang, X. H.; Liu, H.; Wang, N. *China Rubber Indus.* **2013**, *1*, 011.
9. Yin, G. J.; Yang, Y.; Wang, X. P.; Jia, D. M. *China Rubber Indus.* **2006**, *6*, 000.
10. Zanzig, D. J. US Patent 6894122.
11. Cam, L.; Toussaint, J. B. E. *Macromolecules* **2008**, *41*, 7579.
12. Yao, H.; Weng, G.; Liu, Y.; Fu, K.; Chang, A.; Chen, Z. *J Appl. Polym. Sci.* **2015**, *132*, 41986.
13. Weng., G.; Yao., H.; Chang., A.; Fu., K.; Liu., Y.; Chen., Z. *RSC Adv.* **2014**, *4*, 43942.
14. Flory, P. J. Principles of Polymer Chemistry; Cornell University Press, **1953**.
15. Bala, P.; Samantaray, B.; Srivastava, S.; Nando, G. *J. Polym. Sci. Polym. Phys.* **2004**, *92*, 3583.
16. Wu, J.; Huang, G.; Li, H.; Wu, S.; Liu, Y.; Zheng, J. *Polymer* **2013**, *54*, 1937.
17. Peddini, S. K.; Bosnyak, C. P.; Henderson, N. M.; Ellison, C. J.; Paul, D. R. *Polymer* **2015**, *56*, 451.
18. Ding, R.; Leonov, A.; Coran, A. *Rubber Chem. Technol.* **1996**, *69*, 91.
19. Nie, Y.; Huang, G.; Qu, L.; Zhang, P.; Weng, G.; Wu, J. *J. Polym. Sci. Polym. Phys.* **2010**, *115*, 106.
20. Liu, J.; Wu, C.; Zhang, P.; Zhao, S. *J. Macromol. Sci. B* **2008**, *47*, 700.
21. Lei, H.; Huang, G.; Weng, G. *J. Macromol. Sci. B* **2013**, *52*, 94.
22. Rivlin, R.; Thomas, A. G. *J. Polym. Sci.* **1953**, *10*, 291.
23. Lake, G.; Yeoh, O. *J. Polym. Sci. Polym. Phys.* **1987**, *25*, 1190.
24. Weng, G.; Huang, G.; Lei, H.; Qu, L.; Zhang, P.; Nie, Y.; Wu, J. *J. Appl. Polym. Sci.* **2012**, *124*, 4280.